

## CHANGES AND CHALLENGES: GIST, MUTATED c-KIT AND IMATINIB RESISTANCE

Sabrina Pricl<sup>1</sup>, Marco Ferrone<sup>1</sup>, Maria Silvia Paneni<sup>1</sup>, Paolo Cosoli<sup>1</sup>, Maurizio Fermeglia<sup>1</sup>, Marco A. Pierotti<sup>2</sup>, Silvana Pilotti<sup>3</sup>, Elena Tamborini<sup>3</sup>

<sup>1</sup>Molecular Simulation Engineering (MOSE) Laboratory, Department of Chemical Engineering, University of Trieste, Piazzale Europa 1, 34127 Trieste, Italy; <sup>2</sup>Department of Experimental Oncology, Istituto Nazionale per lo Studio e la Cura dei Tumori, via Venezian 1, 20133 Milan, Italy; <sup>3</sup>Department of Molecular Pathology, Istituto Nazionale per lo Studio e la Cura dei Tumori, via Venezian 1, 20133 Milan, Italy

### INTRODUCTION

A new era of targeted cancer therapy was inaugurated with the approval of imatinib mesylate (or STI 571/Gleevec) for the treatment of chronic myeloid leukemia (CML) (1). Imatinib is a phenyl-aminopyrimidine compound, initially identified from a high-throughput screening for inhibitors of protein kinase C and subsequently found to be a potent and selective inhibitor of the Abl, platelet-derived growth factor  $\beta$  receptor, and kit tyrosine kinases. Imatinib binds in a pocket close to the ATP-binding site of the Abl catalytic domain, and effectively inhibits Abl kinase activity in vitro and in vivo at concentrations of 0.1-1.0  $\mu$ M. One year after its approval by FDA and EMEA for CML treatment, in 2001 imatinib was also approved for advanced gastrointestinal stromal tumors (GISTs) chemotherapy. GISTs are the most common mesenchymal tumors of the gastrointestinal tract; they represent a spectrum of tumors, ranging from benign to highly malignant.

In CML, Imatinib is highly effective both in early and late stages of the disease. Nonetheless, several relapses do occur after initial response, despite continued treatment. In patients who developed resistance to imatinib, reactivation of the bcr-abl kinase signaling was observed, due to either a secondary mutation, resulting in a missense substitution of a residue belonging to the drug binding site and critical for binding, or to a progressive BCR-ABL gene amplification (2-6). In GISTs, primary resistance seems to involve at least 15% of patients with advanced disease, and its occurrence could be correlated with different c-kit mutations.

The molecular mechanisms at the bases of imatinib resistance are poorly understood and scarcely investigated. Among a series of patients surgically treated in our Institute all showing clinical/radiological evidence of progressing disease despite of Imatinib treatment, 8 patients were molecularly and biochemically investigated for KIT and PDGFRA gene alterations. None of them showed mutations in PDGFRA gene, and FISH analysis reveal neither KIT or PDGFRA gene amplification (7). The sequencing of the whole coding sequence of KIT gene was performed in the tumoral specimens, revealing activating mutations in exon 11 in all patients. In two patients, two different adjunctive point mutations in KIT gene, one in exon 14 responsible for T670I substitution in the kit protein, and one in exon 13 causing the V654A substitution in the receptor, were detected (8). Biochemical analyses showed c-kit phosphorylation in cells transfected with vectors carrying the specific mutant genes and treated with different doses of imatinib. The modeling of the mutated receptors revealed that both substitutions affect imatinib binding-site, but with different mechanism (9). By the application of molecular simulations we were able to quantify the interactions between the mutated receptors and imatinib, and to propose a molecular rationale for this type of drug resistance at a molecular level.

## MATERIALS AND METHODS

A series of patients surgically treated at Istituto Nazionale per lo Studio e la Cura dei Tumori in Milan, Italy showed evidence of progressing GIST disease despite of Imatinib treatment. Accordingly, they were investigated for the presence of KIT and PDGFRA gene mutations. All patients showed the presence of activating mutations in exon 11. In particular: three patients exhibit the following mutations:  $\Delta 557-558$  in patient 1, V559A in patient 2, and W557G in patient 3. Further, two different point mutations in KIT gene were detected: one in exon 14 responsible for T670I substitution (in patient 1) (7), and one (in two different patients, 2 and 3) in exon 13 causing the V654A substitution (8). None of the patients revealed mutations affecting PDGFRA gene. A highly expressed and phosphorylated kit was detected by immunoprecipitation and Water Blot analysis, despite the fact that all these patients were treated with Imatinib. c-Kit mutants  $\Delta 559$ , T670I and V654A were constructed by site-directed mutagenesis and mutagenesis was checked for success. COS1 cells were transiently transfected with the c-Kit constructs, and were incubated with Imatinib dissolved in DMSO at the indicated doses (1, 3 and 6  $\mu\text{M}$ ) for 8 hours. The proteins were extracted from the transfected cells, and immunoprecipitated using Ab-3 (K45) monoclonal antibody directed against kit receptor; the positive control was a  $\Delta 559$  cell line lysate.

The procedure applied in this work has been described in details in our previous work (6). Accordingly, we will give only a brief outline of the method. All simulations were carried out using the *sander* modulus of AMBER 7.0 (10), and the Cornell et al. (11) force field. The 1.60-Å-resolution coordinates of the kinase domain of c-Kit in complex with Imatinib were obtained from the Brookhaven Protein Data Bank (PDB code 1T46) (12), and used as the starting structure. All crystallographic water molecules were included, and missing hydrogen atoms were added to the protein backbone and side chains with the *parse* module of AMBER 7.0. All ionizable residues were considered in the standard ionization state at neutral pH. The missing force field parameters for the inhibitor were taken from our previous work (6). Mutations T670I and V654A were introduced into the wild type structure of c-Kit/Imatinib complex using the Biopolymer module of Insight II (v. 2001, Accelrys Inc., San Diego, CA, USA) by swapping the mutant residue into the specific site, according to a dedicated and well-validated procedure (6,13). To set up each resulting complex for the simulation, we adopted following ansatz: first, each complex was immersed in a sphere of TIP3P water molecules (14). To achieve electroneutrality, a suitable number of counterions were added, in the positions of largest electrostatic potential, as determined by the module *cion* within AMBER 7.0. All three systems (wild type, T670I and V654A c-Kit/Imatinib complexes, respectively) were then minimized and equilibrated with an *ad hoc* protocol (6). Following minimization, each system was heated up to 300 K in three stages by coupling to an external bath (15). Each hydrated complex was then further equilibrated for 50 ps at 300 K, and we continued each simulation for other 400 ps at 300 K, a time necessary for the estimation of the free energy of binding (*vide infra*). The MD simulations were performed using an integration time step of 2 fs, and the application of the SHAKE algorithm (16).

All energetic analysis was done for only a single MD trajectory of each c-Kit/Imatinib complex considered, with unbound protein and substrate snapshots taken from the snapshots of that trajectory. According to the so-called Molecular Mechanics/Poisson-Boltzmann Surface Area method (MM/PBSA) (17), the binding free energy between Imatinib and c-Kit can be calculated as:

$$\Delta G_{\text{bind}} = \Delta E_{\text{MM}} + \Delta G_{\text{solv}} - T\Delta S \quad (1)$$

where:

$$\Delta G_{\text{solv}} = \Delta G_{\text{PB}} + \Delta G_{\text{NP}} \quad (2)$$

$\Delta E_{\text{MM}}$  denotes the sum of molecular mechanics (MM) energies of the molecules, and can be further split into contributions from electrostatic ( $E_{\text{EL}}$ ) and van der Waals ( $E_{\text{vdW}}$ ) energies:

$$\Delta E_{\text{MM}} = \Delta E_{\text{EL}} + \Delta E_{\text{vdW}} \quad (3)$$

The terms in equation (3) were calculated by using the *cnal* and *anal* modules of AMBER 7.0.  $\Delta G_{\text{solv}}$  was evaluated with the Poisson-Boltzmann (PB) approach (17). The non polar solvation contribution to solvation  $\Delta G_{\text{NP}}$  was calculated (18) as  $\Delta G_{\text{NP}} = \gamma (\text{SASA}) + \beta$ , in which  $\gamma = 0.00542 \text{ kcal}/\text{\AA}^2$ ,  $\beta = 0.92 \text{ kcal/mol}$ , and SASA is the solvent-accessible surface estimated with the MSMS program (19). Finally, the normal-mode analysis approach was followed to estimate the last parameter, i.e. the change in solute entropy upon association  $-T\Delta S$  (19).

The free energy of binding difference  $\Delta\Delta G_{\text{bind}}$  between wild-type and each c-Kit mutant and Imatinib was calculated as:

$$\Delta\Delta G_{\text{bind}} = \Delta G_{\text{bind}}(\text{wild-type}) - \Delta G_{\text{bind}}(\text{mutant}) \quad (4)$$

Accordingly, negative  $\Delta\Delta G_{\text{bind}}$  values indicate highly unfavorable substitutions at the considered position, and vice versa.

## RESULTS AND DISCUSSION

Based on antiphosphotyrosine immunoblot analysis with cells treated with 3 different doses of the drug, Kit/T670I and Kit/V654A clearly were resistant to Imatinib compared to the Kit/ $\Delta$ 559 Imatinib-sensitive mutation. Kit/T670I resulted to be phosphorylated and thus insensitive to the drug at all the doses, while Kit/V564A resulted totally inhibited at 6  $\mu\text{M}$  of Imatinib. Since in all the patients in which these aminoacidic substitutions were observed, the corresponding DNA mutations were on the allele which carried also the activating exon 11 Kit mutation, we investigated the effect of their presence on an activated Kit receptor. Accordingly, we introduced the T670I and the V654A mutations into the KIT/ $\Delta$ 559 mutant. The resulting KIT/ $\Delta$ 559/T670I and KIT/ $\Delta$ 559/V654A mutants were transiently expressed in COS1 cells. Western blot analysis showed that KIT/ $\Delta$ 559/T670I was resistant to Imatinib at all the concentrations while KIT/ $\Delta$ 559/V654A resulted inhibited at the dose of 6  $\mu\text{M}$  of Imatinib.

Mutating T into I at position 670 in the ATP-binding site of the c-Kit kinase domain results in a calculated  $\Delta\Delta G_{\text{bind}}$  for Imatinib equal to  $-3.84 \text{ kcal/mol}$ . Both nonbonded interaction components of the free energy of binding strongly decrease in the presence of the mutated isoform ( $\Delta\Delta E_{\text{MM}} = -5.87 \text{ kcal/mol}$ ). This marked decreased affinity for this mutant with respect to Imatinib has to be ascribed to the molecular dimensions of the inhibitor which are too big to result in a snug fit within the pocket formed at the N- and C-lobe interface of the inactive structure of the kinase. Indeed, the phenyl ring of Imatinib packs too tightly between the aliphatic chains of D810, E640 and L644, while the piperazine ring makes no specific interactions with the protein and fits in a shallow pocket bounded by V643, C788, I789, H790, R791 and D810 (Figure 1).

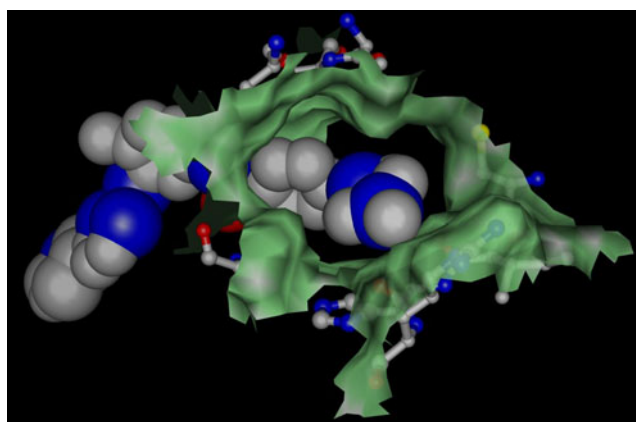


**Figure 1** - Detail of Imatinib (atom-colored space-filling rendering) docked into the T670I c-Kit model showing the side chains of residues E640, V643, L644, C788, I789, H790, R791 and D810 (atom-colored stick-and-ball rendering). The green shadow, representing the amino acid molecular surface, highlights the narrow space available to the inhibitor.

As seen for the analogous mutation T315I in the ABL kinase domain (6), in a sort of a domino effect the substitution of this single residue in this position induces several, sometimes substantial modifications in the conformation of other residues, both belonging to the binding site and the surrounding areas, as a direct consequence of the different position assumed by Imatinib in the binding site. The topical, stabilizing hydrogen bond between the aminopyridine nitrogen of Imatinib and the side chain O $\gamma$ 1 atom of the gatekeeper residue T760 does no longer exist, and is not replaced by any similar, favorable interaction. Moreover, the greater molecular volume of isoleucine (I) side chain with respect to threonine (T) induces Imatinib to assume a slightly modified position within the pocket to alleviate sterical unfavorable interferences. Finally, the active kinase structure is characterized by a critical salt link between a conserved C-helix D640 and K623 that orients the lysine side chain for interactions with the nucleotide phosphate (20). This salt link, absent in the trajectory of the wild-type KIT/Imatinib, is present in the corresponding MD simulation of the T670I mutant/Imatinib complex, with an average dynamic length of 2.8 Å.

Residue V654 is in KIT kinase domain 1, and is notably conserved among other kinases such as Abl, Src, Hck, Flt3, and PDGFR. Mutating V to A at position 654 in the ATP-binding domain of the KIT results in calculated  $\Delta\Delta G_{\text{bind}}$  for Imatinib of -1.52 kcal/mol. Indeed, exchanging V to A decreases the degree of surface complementarity between KIT and the inhibitor, due to the smaller A dimensions, which account for the most part of the nonbonded interactions ( $\Delta\Delta E_{\text{vdW}} = -1.08$  kcal/mol, and  $\Delta\Delta E_{\text{MM}} = -1.27$  kcal/mol). Contrarily to what observed for the T670I mutation, in fact, both the electrostatic and solvation terms remain almost unaffected, as expected for a conservative substitution. We can conclude that this decrease in binding affinity is then substantially due to the loss of packing interaction (i.e., cavity formation) in the native state of the alanine-containing variant. We can then estimate the destabilizing effect of cavity formation per one carbon (methyl group) atom. The V to A substitution removes two carbon atoms; the calculated  $\Delta\Delta G_{\text{bind}}$  for V654A mutant disfavors the mutant by 1.52 kcal/mol, resulting in a destabilization of approximately 0.8 kcal/mol per carbon atom upon cavity formation. Replacing V with A at position 654 further reflects only in a slight alteration of some other imatinib contact points (E640, T670, C673, F811) and some ATP-binding residues (K623, E671). In particular, the readjustment of K623 results in a decreased interaction of this residue with E640 in C-helix (Figure 2). Finally, V654 is engaged in two

stabilizing hydrogen bonds interactions. The former involves the C=O backbone group of V654 and the bridging water 956 on one side (ADL = 2.85 Å), and the same water molecule and the C=O backbone group of G648 on the other (ADL = 2.81 Å). The second H-bond involves the NH backbone moiety of V654 and the backbone C=O of I808, with an ADL of 3.03 Å. Interestingly, the same interactions are present in our MD trajectory of the A654 mutant, the former involving the same functional groups and water 1011 (ADL = 2.90 Å and 2.83 Å, respectively), and the second being characterized by ADL = 2.93 Å. Since these H-bonds involve only backbone atoms of the residue at position 654, it is not surprising that the same two favorable interactions are preserved in our simulation of the A654 variant.

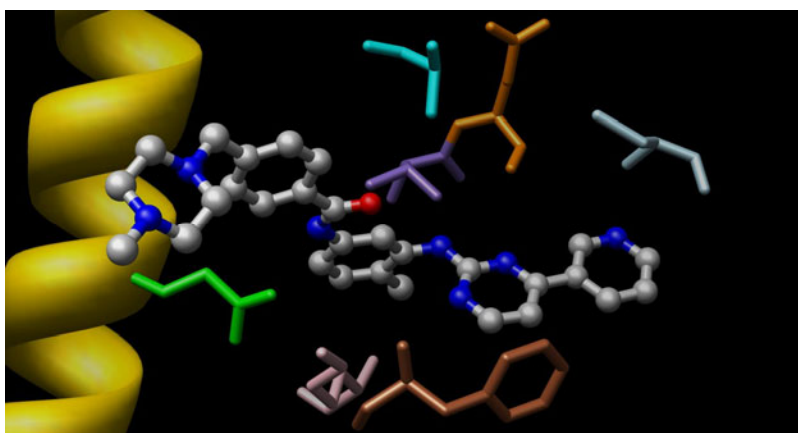


**Figure 2** – Details of the interaction of A654 and some Imatinib contact points and ATP-binding residues. All residues are in stick rendering (color code: K623 pink, E640 green, A654 cyan, T670 purple, E671 orange, C673 light blue). Imatinib is in atom-colored stick-and-ball rendering. C-helix is in gold ribbon rendering.

## CONCLUSIONS

In this work we reported the biochemical characterization coupled with the molecular modeling of two c-Kit mutations, T670I and V654A, detected in three different patients with clinical and radiological symptoms of progressing disease despite Imatinib treatment. We demonstrated how the presence of A (alanine) in position 654 or I (isoleucine) in position 670 is actually responsible for the acquired resistance to Imatinib. For both the substitutions in fact, at 3 $\mu$ M of the drug the detection of phosphorylated bands indicates the occurrence of activated receptors. Interestingly, the single and double mutant V654A resulted unphosphorylated and thus inhibited at 6  $\mu$ M of Imatinib, while the single and double mutant T670I did not. A reason of this behavior, at a molecular level, can be found in the results obtained from the molecular dynamic simulations performed on the complex of Imatinib with wild-type and both mutated Kit receptors. In fact, the reported values of the difference in the calculated free energies of binding of Imatinib and the two mutant proteins, clearly suggest that two different mechanisms should lie at the base for the lower inhibitor affinity. The  $\Delta\Delta G_{\text{bind}}$  obtained for the Kit/T670I mutant is -3.84 kcal/mol, suggesting that the replacement of the polar residue T with the neutral I induce a substantial deformation of the binding pocket. Accordingly, the missing hydrogen bond between I670 and Imatinib is not the only leading cause for drug binding failure to the protein. In utter analogy with what observed by us for the homologous residue T315 in the c-ABL kinase domain (6), this failure instead results from a domino effect induced by the

conformational readjustment necessary to accommodate the mutant residue and which involves several other important drug contact points. On the contrary, the smaller  $\Delta\Delta G_{\text{bind}}$  value obtained for the V654A mutant is in line with a replacement of a hydrophobic residue into another of smaller size. Vast amount of structural data on various mutant proteins suggest that single site amino acid substitutions, especially in case of conservative replacements, do not affect the global structure of proteins. In other words, mutant proteins usually retain overall structures that are very similar to those of their wild type parents. In some cases, there are no conformational alterations, and the structure remains completely unchanged. In the rest of the cavity creating variants, there are some movements in the position of atoms leaning the newly created cavity, but in each case the cavity remained in the structure of the variant. Clearly this is the case of the KIT/V654A mutant: in this scenario, a “cavity creating” amino acid substitution (V→A) at a largely buried site such as position 654 in KIT does not lead to dramatic structural changes that completely alters or eliminates the cavity, but has effect only on the structure in the vicinity of the substitution site.

All these observations are in line with our experimental evidences that the Kit/T670I mutant remains insensible to Imatinib at all concentrations testes, whereas 6  $\mu\text{M}$  Imatinib is able to switch off the phosphorylation activity of the Kit/V654A mutant protein. Interestingly, the V654A mutation was detected in a patient treated with 400 mg/die of Imatinib. It would have been interesting to observe the clinical and radiological evolution of this tumor if the patient would have been treated with Imatinib at 800 mg/die. Based on our data in fact, the effect of this mutation might be subverted by a dose escalation of the inhibitor and it would be expected to recapture a clinical response.

## ACKNOWLEDGMENTS

Authors gratefully acknowledge the generous financial support received from the Italian Association for Cancer Research (AIRC), grant “Analysis of response mechanisms to imatinib in soft tissues sarcomas”, 2005.

## REFERENCES

1. Druker BJ, Tamura S, Buchdunger E, Ohno S, Segal GM, Fanning S, et al. *Nat Med* 1996;**2**:561.
2. Corbin AS, Buchdunger E, Furet P, Druker BJ. *J Biol Chem* 2001;**277**:32214-32219.
3. Shah NP, Nicoll JM, Nagar B, Gorre ME, Paquette RL, Kuriyan J, et al. *Cancer Cell* 2002;**2**:117.
4. Ricci C, Scappini B, Divoky V, Gatto S, Onida F, Verstovsek S, et al. *Cancer Res* 2002;**62**:5995.
5. von Boubnoff N, Schneller F, Peschel C, Duyster J. *Lancet* 2002;**359**:487.
6. Pricl S, Fermeglia M, Ferrone M, Tamborini E. *Mol Cancer Ther* 2005;**4**:1167.
7. Tamborini E, Bonadiman L, Greco A, Albertini V, Negri T, Gronchi A, et al. *Gastroenterology* 2004;**127**:294.
8. Tamborini E, Gabanti E, Lagonigro MS, Negri T, Pilotti S, Pierotti MA, Pricl S. *Cancer Res*. 2005;**65**:1115.
9. Pricl S, Tamborini E, Lagonigro MS, Negri T, Pilotti S, Pierotti MA. *JNCI* 2005, in press.

10. Case DA, Pearlman DA, Caldwell JD, et al. AMBER 7, University of California, San Francisco, CA USA, 2000.
11. Cornell WD, Cieplak P, Bayly CI, et al. *J Am Chem Soc* 1995;**117**:5179.
12. Mol CD, Dougan DR, Schneider TR, et al. *J Biol Chem* 2004;**23**:31655.
13. Reyes CM, Kollman PA. *J Mol Biol* 2000;**295**:1.
14. Jorgensen WL, Chandrasekhar J, Madura JD, Impey RW, Klein ML. *J Chem Phys* 1983;**79**:926.
15. Berendsen HJC, Postma JPM, van Gunsteren WF, DiNola A, Haak JR. *J Chem Phys* 1984;**81**:3684.
16. Ryckaert JP, Ciccotti G, Berendsen HJC. *J Comp Phys* 1977;**23**:327.
17. Srinivasan J, Cheatham TE III, Cieplak P, Kollman PA, Case DA. *J Am Chem Soc* 1998;**120**:9401.
18. Gilson MK, Sharp KA, Honig B. *J Comput Chem* 1987;**9**:327.
19. Sanner MF, Olson AJ, Spehner JC. *Biopolymers* 1996;**38**:305.
20. Mol CD, Lim KB, Sridhar V, et al. *J Biol Chem* 2003;**278**:31461.